

MEASURING 3D LEFT VENTRICULAR STRAIN FROM UNWRAPPED HARMONIC PHASE

Bharath Ambale, Thomas S. Denney Jr.

ECE Department
Auburn University
Auburn, AL USA

Himanshu Gupta, Steven Lloyd, Louis Dell'Italia

Division of Cardiovascular Disease
University of Alabama at Birmingham
Birmingham, AL USA

ABSTRACT

This paper presents a method for measuring 3D left ventricular (LV) strain from phase unwrapped harmonic phase (HARP) images derived from tagged cardiac magnetic resonance imaging (MRI). Limited user interaction is needed, but, in contrast to existing techniques, 3D strains can be measured over the entire LV. In addition, unwrapped phase is more robust to interframe motion since it only requires that the average interframe deformation be less than one-half tag spacing. The unwrapped-phase-derived strains were validated on a set of 30 human studies by comparing them to strains estimated by a feature-based technique. The standard deviation of the difference between strains measured by the two methods was less than 5% of the average of the strains from the two methods.

Index Terms— Phase unwrapping, tagged magnetic resonance imaging, strain, left ventricle

1. INTRODUCTION

Parameters of cardiac left ventricular (LV) mechanical function are important for diagnosing and managing patients with heart disease and assessing the efficacy of therapies over time. Tagged magnetic resonance imaging (MRI) is an established method for measuring parameters of LV deformation and strain. Tagged MRI spatially modulates the longitudinal magnetization of the underlying tissue before image acquisition. The result is a periodic tag pattern that deforms with the tissue as shown in Fig. 1(a). Several techniques have been developed to measure LV deformation and strain from the deformation of the tag pattern. These techniques include feature-based (FB) methods and harmonic phase (HARP)-based methods.

In HARP [1] analysis, the tag pattern deformation is measured by the local change in phase of the tag pattern. The tag pattern modulates the signal intensity of the image producing a series of peaks in the Fourier domain as shown in Fig. 1(b). One of these peaks is filtered out and inverse Fourier transformed to produce a HARP phase image. The HARP phase at a point in the image is a material property of the underlying tissue and can be tracked through the image sequence or used to compute 2-D strain. 3-D LV deformation can be measured with HARP analysis by using the HARP phase in a collection of slices to track a 3D mesh through an image sequence [2]. HARP analysis is fast and requires little user intervention, but the HARP phase is wrapped (i.e. can only be measured modulo 2π) as seen in Fig. 1(c). This wrapping can cause tracking problems if a region of the tissue deforms more than one-half tag spacing (i.e. a phase shift of more than π) between timeframes. Deformations of this magnitude are possible in both healthy and diseased hearts.

In this paper, a method is presented for measuring 3D LV deformation and strain from HARP images using phase unwrapping. Phase unwrapping involves adding multiples of 2π to the wrapped phase so that the unwrapped phase is continuous. Phase unwrapping is used in other imaging modalities such as SAR interferometry and optics as well as MRI [3]. The phase unwrapping algorithm in this paper requires more user interaction than [2], but the unwrapping algorithm can measure strains in entire LV, whereas the method in [2] can only measure the middle third. In addition, the phase unwrapping approach is more robust to interframe motion than techniques such as [2] that are based on tracking wrapped phase. With unwrapped phase, points can be tracked through an image sequence as long as the deformation between timeframes is less than half a tag spacing. Compared to other feature-based methods, displacement measurements from unwrapped HARP phase images are significantly more dense than those obtained from tracking tag lines or tag intersections, potentially resulting in more accurate estimates of strain.

This paper is organized as follows. The phase unwrapping algorithm and strain reconstruction is presented in Sections 2 through 3. Experimental results and conclusions are presented in Sections 4 and 5.

2. UNWRAPPING HARP PHASE

Phase unwrapping involves adding integer multiples of 2π to each pixel in the wrapped image so that 1) the unwrapped phase is continuous and 2) if the unwrapped phase is re-wrapped, the result is equivalent to the original wrapped image. In this paper, phase is unwrapped only inside the LV wall. Several phase unwrapping algorithms have been proposed [4]. In this paper, a path-following method is used where phase is unwrapped along a path in the image from one pixel to another. If the phase is unwrapped correctly, the phase of the destination pixel is independent of the path taken. Two main issues arise with this approach: how to choose the path and how to handle regions of inconsistent phase. The path is chosen by a quality-guided method. Phase inconsistencies are called residues and are handled by introducing branch cuts. These methods are described in detail in the following sections.

2.1. Quality-Guided Phase Unwrapping

In path-following methods, it is necessary to determine a path that visits each pixel of interest. The phase is unwrapped along this path. In quality-guided phase unwrapping [4], a starting point is chosen and the next pixel visited is the neighbor with the highest quality. This process is repeated until all pixels of interest have been processed. In this paper, quality was defined as the reciprocal of the

This work was supported by NIH grant P50-HL077100.

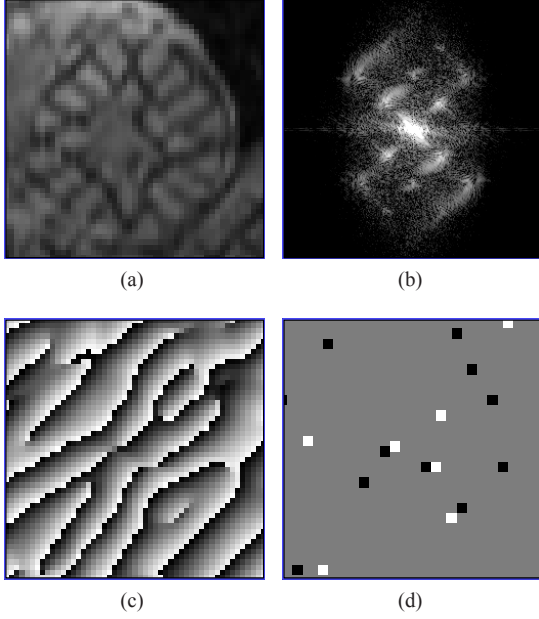


Fig. 1. (a) a tagged short-axis image acquired near end-systole in a normal human. (b) the Fourier transform magnitude of (a). (c) a HARP image obtained by bandpass filtering around one of the peaks in (b). (d) negative(black) and positive(white) residues in the HARP image in (c).

phase difference variance [4], which is given by

$$z_{mn} = \frac{\sqrt{\sum(\Delta_{i,j}^x - \Delta_{m,n}^x)^2} + \sqrt{\sum(\Delta_{i,j}^y - \Delta_{m,n}^y)^2}}{9}, \quad (1)$$

where each sum is over a 3×3 window centered at the pixel (m, n) . The terms $\Delta_{i,j}^x$ and $\Delta_{i,j}^y$ are the wrapped phase derivatives and $\Delta_{m,n}^x$ and $\Delta_{m,n}^y$ are the average of the derivatives in the 3×3 window.

2.2. Residues

Residues are the cause for inconsistencies in the HARP phase image. Residues arise out of singularities in the wrapped phase or zeros in the complex function used to derive the wrapped phase. A simple method for identifying the residues is by summing the phase differences around a 2×2 block around a pixel.

The sum of the phase differences around the 2×2 block should be zero. If the phase difference sum is not zero, then a residue is said to be present. Residues add up to either $+2\pi$ or -2π and are respectively known as positive or negative residues. Residues are a major problem in phase unwrapping, and the presence of residues means that the unwrapping is path dependent. The residues are marked black and white for negative and positive residues respectively as seen in Fig. 1(d). The number of residues is clearly larger in the outer areas where there is air and areas of the image with large motion compared to the areas with static tissues as seen in the original MRI image in Fig. 1(a).

Removal of residues is essential to obtain unwrapped phase without any discontinuities. In this paper, the residue compensation method [4] is used where residues are removed by connecting

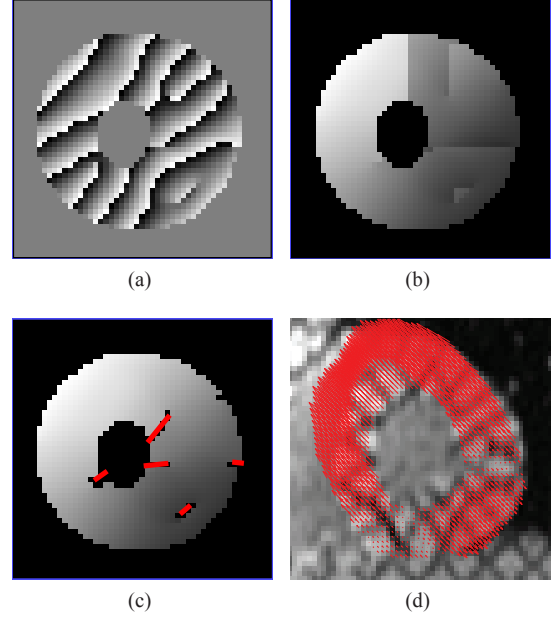


Fig. 2. Phase unwrapping example: (a) wrapped HARP phase; (b) unwrapped image without branch cuts; (c) unwrapped phase with branch cuts; (d) 1-D displacements measured from the unwrapped phase.

residues with branch cuts. An unwrapping path is not allowed to cross a branch cut. Either a positive residue is connected to a negative residue, or, if only a positive residue is unwrapped, a residue is connected to a point outside the region. Once the branch cuts are placed, the unwrapping is path independent and the quality-guided method is used to unwrap the images. The problem, of course is which residues to connect. It is common to see positive and negative residues next to each other in the image (see Fig. 1(d)). These are known as dipoles and can be automatically removed with a branch cut.

How to connect non-dipole residues, however, is a difficult problem. In cases where there are an equal number of positive and negative residues, automated methods have been proposed that, for example, minimize the average branch cut length [5], but there is no guarantee that the branch cuts are properly placed. As a result, the user must place the branch cuts interactively. This can be done quickly with a graphical user interface (GUI). Fig. 2 shows an example. Fig. 2(a) shows the wrapped image phase. Residues occur where the two phase lines meet (1 o' clock and 8 o' clock) and the premature ending of the phase line near the epicardium (3 o' clock). Without branch cuts, the unwrapped phase is discontinuous (Fig. 2(b)). Fig.2(c) shows the user-placed branch cuts and the resulting unwrapped phase.

Each image is unwrapped independently, and the starting point for phase unwrapping may be different in each image. As a result, the unwrapped phases in two adjacent timeframes may differ by an integer multiple of 2π . This difference can be corrected by adding the integer multiple of 2π to all unwrapped phase in the current timeframe. The multiple is chosen to minimize the L_1 norm of all displacements between the current and previous frames. Note that this correction assumes that the L_1 norm of the unwrapped phase difference between consecutive frames is less than π , which corresponds

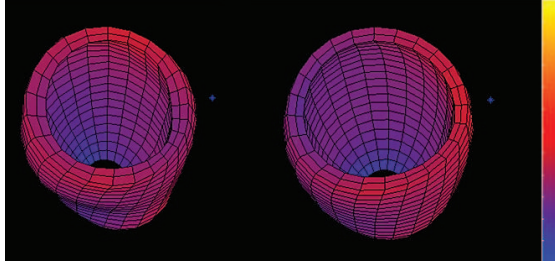


Fig. 3. Maps of circumferential (E_{cc}) strain using unwrapped phase (left) and feature-based (right) methods. Strains are mapped from blue = -30% to yellow = 30%

to one-half of the tag spacing. Also, interframe deformation of more than one-half tag spacing in a localized region or regions will not affect the unwrapped phase as long as the average deformation is less than one-half tag spacing.

3. MOTION AND STRAIN ESTIMATION

Once the phases have been unwrapped and aligned, 1-D displacements can be measured from each pixel in the myocardium similar to those measured from tag-line tracking data [6]. Each 1-D displacement measurement is the displacement of the point back to its undeformed position along a line perpendicular to the tag plane (see [6] for details). To compute these displacements, an estimate of the undeformed phase plane must be computed. The undeformed phase plane is estimated by fitting a plane to the unwrapped phase plane in the first timeframe in a given slice. This computation is analogous to the one performed in tag-line-based analysis to determine the undeformed tag line center and spacing. There can be some motion between the time the tags are applied and the acquisition of the first image, but this is usually small. A similar assumption is used in Pan [2]. Since tag lines are parallel when they are applied, the undeformed phase plane can be specified by the 1-D linear equation $\phi_u(s) = ms + b$, where s is a parameter that sweeps out a line perpendicular to the tag line. Let s_d correspond to a point in a deformed image. The linear equation can be solved to determine s_u , the point in the undeformed image with the same phase. The displacement measurement is then $d = s_d - s_u$. This procedure is repeated for each tag line direction in the image. Fig. 2(d) shows an example of displacement measurements measured from a short-axis slice of a normal human volunteer at end-systole.

Both the phase alignment and displacement measurement steps require that the LV wall be segmented in each slice and time of interest. Usually only the systolic timeframes are analyzed since, after end-systole, the tag lines are often too faded for reliable analysis. In this algorithm, the myocardium is segmented based on LV contours drawn by the user at end-diastole (ED) and end-systole (ES). Non-rigid registration [7] is used to propagate ED and ES contours to the systolic time frames. ED contours are used in almost all tagged MRI analysis algorithms to define a material-point mesh or other set of points of interest. ES contours were included because they improve the ability of the propagated contours to distinguish between papillary muscles and the LV wall.

The 1-D displacement measurements and a material-point mesh automatically constructed from the ED contours are used to compute 3-D LV deformation and strain in each systolic timeframe. The deformation and strain are reconstructed using the Affine Prolate

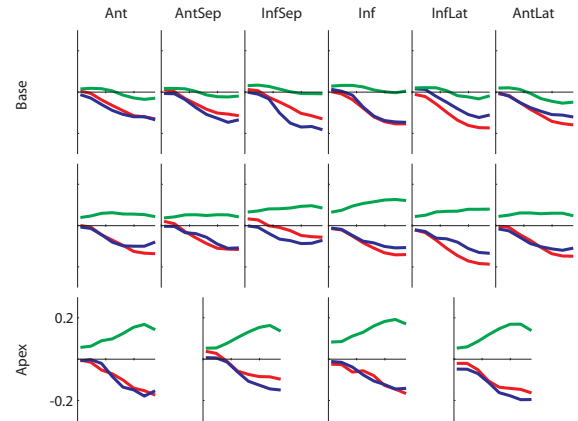


Fig. 4. Circumferential strain (red), longitudinal strain (blue), and rotation in radians (green) for a representative normal human volunteer versus time (10 to 275 msec) computed using the phase unwrapping algorithm.

Spheroidal B-Spline (APSB) method in [8], which fits a B-spline deformation model defined in prolate-spheroidal coordinates to the displacement measurements. First, a backward fit is performed in each timeframe that maps each point back to its undeformed position. A series of forward fits are then performed to compute the trajectory of each point in the material-point mesh through systole. 3-D strain is computed by spatially differentiating the deformation model.

4. EXPERIMENTS

The procedure was tested on 30 human studies from different pathologies (10 normals, 10 patients with myocardial infarction, and 10 patients with hypertension). All participants underwent MRI on a 1.5T MRI scanner (GE, Milwaukee, WI) optimized for cardiac application. Tagged images were acquired in standard views (2 and 4 chamber long axis and short axis) with a fast gradient-echo cine sequence with the following parameters: FOV = 300 mm, image matrix = 224x256, flip angle = 45, TE = 1.82ms, TR = 5.2ms, number of cardiac phases = 20, slice thickness = 10 mm. A 2D spatial modulation of magnetization (FGR-SPAMM) tagging preparation was done with a tag spacing of 7 pixels. This protocol resulted in 2 long-axis slices and, on average, 12 short-axis slices per study.

All studies were processed using the unwrapped-phase (UP) technique described above, which was implemented in MATLAB. First, LV contours were drawn at ED and ES and automatically propagated to all systolic timeframes. Unwrapping all images in a study took less than a minute on a 2.6GHz Core2 Duo processor with 4Gb of memory. Approximately 10 minutes per study of user interaction were required to resolve residues. Phase alignment and strain reconstruction took approximately 5 minutes per study.

Fig. 3 shows maps of 3D circumferential strain (E_{cc}) in a representative normal human volunteer computed from the UP method and a feature-based (FB) method based on tag line tracking [8]. The same material-point mesh and deformation model was used to reconstruct strain in both methods. Note that strain is computed in the entire LV, except the apex which is typically not included in this type

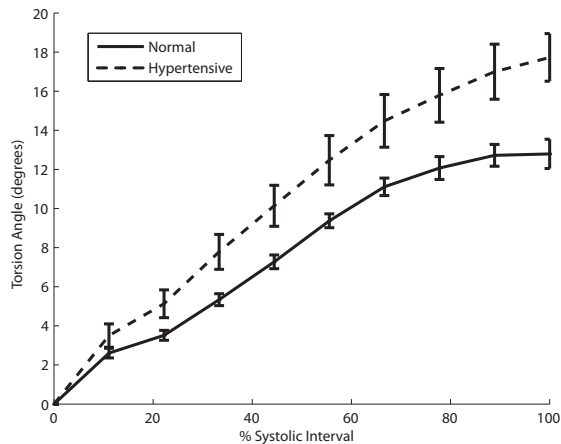


Fig. 5. Torsion angle (rotation of the apex relative to the base) versus % systolic interval averaged over 10 normal human volunteers and 10 patients with hypertension. Error bars represent \pm one standard error.

of analysis. The strain maps are quite close. The primary difference is that the UP map demonstrates more torsion (rotation of the apex relative to the base) than the FB map. This difference is probably because the UP method provides more dense displacement measurements (two per pixel in grid-tagged images), whereas the FB method only provides displacement measurements at each tag line point.

Table 1 shows statistics of the difference between the UP and FB methods. In all strains in Table 1, the difference standard deviation is less than 5% of the average of the two methods. The correlation between the methods is strongest in circumferential and (signed) minimum principal strain because circumferential deformation is most densely measured in this imaging protocol. Only two long-axis images are acquired, so the correlation in longitudinal strain (E_{ll}) and torsion is lower, but still good. In fact, the UP method may provide more accurate measurements of E_{ll} , torsion and other strains than the FB method, but further investigation is needed to support this claim.

Fig. 4 shows plots of E_{cc} , E_{ll} , and rotation angle vs % systolic interval in a representative normal human volunteer. The evolution of all three parameters agree with previous measurements in the literature. E_{cc} and E_{ll} increase through systole and tend to be higher on the lateral wall than on the septal wall. The rotation plots show a small counter-clockwise rotation of the base and a larger clockwise rotation of the apex.

Fig. 5 shows a plots of torsion versus time averaged over 10 normal human volunteers and 10 patients with hypertension. The hypertensive patients show an increase in torsion, which has been reported in the clinical literature [9].

5. CONCLUSIONS

The unwrapped-phase (UP) method was presented for measuring 3D strain from tagged MRI. Strains computed using UP demonstrated excellent agreement with an existing feature-based method. Compared to other HARP-based techniques, the UP method requires that an additional timeframe be contoured, but this additional timeframe provides a significant increase in propagated contour accuracy.

| Measurement | E_{cc} | E_{ll} | E_{min} | Torsion |
|-----------------|----------|----------|-----------|---------|
| Mean Difference | -0.0026 | -0.0035 | 0.0035 | 0.5789 |
| Diff. Std. Dev. | 0.0123 | 0.0166 | 0.0134 | 1.5110 |
| CV(%) | 2.27 | 3.98 | 1.78 | 3.95 |
| Correlation | 0.96 | 0.91 | 0.93 | 0.84 |

Table 1. Comparison of strains and torsion computed using the unwrapped phase (UP) and feature-based (FB) methods. Difference = FB - UP. CV: coefficient of variation.

Some user interaction is also required to resolve phase-unwrapping residues (typically around the apex), but the UP method can compute strains in the entire LV instead of just the middle third. In future work, we plan to investigate ways of automatically resolving residues and perform a comparison of the UP and feature-based methods to determine which method is more accurate in estimating strains.

6. REFERENCES

- [1] N. F. Osman and E. R. McVeigh, "Imaging heart motion using harmonic phase MRI," *IEEE Trans Med Imag*, vol. 19, no. 3, pp. 186–202, March 2000.
- [2] L. Pan, J. Prince, J. Lima, and N. Osman, "Fast tracking of cardiac motion using 3D-HARP," *IEEE Trans Biomed Eng*, vol. 52, no. 8, pp. 1425–1435, Aug. 2005.
- [3] B. S. Spottiswoode, X. Zhong, A. T. Hess, C. M. Kramer, E. M. Meintjes, B. M. Mayosi, and F. H. Epstein, "Tracking myocardial motion from cine DENSE images using spatiotemporal phase unwrapping and temporal fitting," *IEEE Trans Med Imag*, vol. 26, no. 1, pp. 15–30, Jan. 2007.
- [4] D. C. Ghiglia and M. D. Pritt, *Two-dimensional phase unwrapping: theory, algorithms, and software*. New York: Wiley, 1998.
- [5] H. Zebker and Y. Lu, "Phase unwrapping algorithms for radar interferometry: Residue-cut, leastsquares, and synthesis algorithms," *J Opt Soc Amer*, 1998.
- [6] T. Denney Jr. and J. Prince, "Reconstruction of 3-D left ventricular motion from planar tagged cardiac MR images: an estimation theoretic approach," *IEEE Tran Med Imag*, vol. 14, no. 4, pp. 625–635, Dec. 1995.
- [7] W.Feng, H.Gupta, S.Lloyd, L.Dell'Italia, and T. S. Denney, "Myocardial contour propagation in cine cardiac MRI," in *Joint Annual Meeting ISMRM-ESMRMB*, May 2007, p. 766.
- [8] J. Li and T. S. Denney Jr., "Left ventricular motion reconstruction with a prolate spheroidal B-spline model." *Phys Med Biol*, vol. 51, no. 3, pp. 517–537, Feb 2006.
- [9] M. Stuber, M. B. Scheidegger, S. E. Fischer, E. Nagel, F. Steineemann, O. M. Hess, and P. Boesiger, "Alterations in the Local Myocardial Motion Pattern in Patients Suffering From Pressure Overload Due to Aortic Stenosis," *Circulation*, vol. 100, no. 4, pp. 361–368, 1999.